Bacteriorhodopsin's Intramolecular Proton-Release Pathway Consists of a Hydrogen-Bonded Network†

Robin Rammelsberg, Gregor Huhn, Mathias Lübben, and Klaus Gerwert*

Lehrstuhl für Biophysik, Ruhr-Universität Bochum, D-44780 Bochum, Germany

Received July 14, 1997; Revised Manuscript Received February 2, 1998

ABSTRACT: In its proton-pumping photocycle, bacteriorhodopsin releases a proton to the extracellular surface at pH 7 in the transition from intermediate L to intermediate M. The proton-release group, named XH, was assigned in low-temperature FT-IR studies to a single residue, E204 [Brown, L. S., Sasaki, J., Kandori, H., Maeda, A., Needleman, R., and Lanyi, J. K. (1995) *J. Biol. Chem. 270*, 27122−27126]. The time-resolved room-temperature step-scan FT-IR photocycle studies on wild-type and E204Q-, and E204D-mutated bacteriorhodopsin, which we present here, show in contrast that the FT-IR data give no evidence for deprotonation of E204 in the L-to-M transition. Therefore, it is unlikely that E204 represents XH. On the other hand, IR continuum absorbance changes indicate intramolecular proton transfer via an H-bonded network to the surface of the protein. It appears that this H-bonded network is spanned between the Schiff base and the protein surface. The network consists at least partly of internally bound water molecules and is stabilized by E204 and R82. Other not yet identified groups may also contribute. At pH 5, the intramolecular proton transfer to the surface of the protein seems not to be disturbed. The proton seems to be buffered at the surface and later in the photocycle released into the bulk during BR recovery. Intramolecular proton transfer via a complex H-bonded network is proposed to be a general feature of proton transfer in proteins.

Proton-transfer reactions play a crucial role in the catalytic function of many enzymes. The light-driven proton pump bacteriorhodopsin (bR)[1] represents an excellent system to study the proton-transfer mechanism in membrane proteins (*2*). The seven α-helices of bR span the membrane of the archaebacterium *Halobacterium salinarium.* The chromophore retinal is bound via a protonated Schiff base to K216, as in all retinal proteins (*3*). An atomic structural model based on cryoelectron microscopic studies has been proposed (*4*, *5*). After light excitation, bR undergoes a proton-pumping photocycle with the intermediates K, L, M, N, and O in order of their appearance (*6*). The different intermediates are characterized by their UV−vis (*7*), resonance-Raman (*8*), and infrared spectra (*9*). Crucial events in the pump mechanism are the light-induced *all-trans* to 13-*cis* retinal isomerization in the BR-to-K transition (*10*), the deprotonation of the Schiff base and the corresponding protonation in the L-to-M transition of the nearby D85 (*11*−*15*), the reprotonation of the Schiff base by D96 in the M-to-N transition (*13*, *14*), and the 13-cis to *all-trans* reisomerization in the N-to-O transition (*16*).

At pH 7, a proton appears at the extracellular surface of bR with a time constant of about 80 μs (*17*−*20*). Then, the proton is released into the bulk medium about 1 ms delayed. The pK_a of the group that releases the proton from the surface into the bulk was determined to be 5.8 in the M intermediate (*21*, *22*). Below pH 5.8, proton release into the bulk occurs during BR recovery after proton uptake, which takes place during M decay. Because the proton of the Schiff base is transferred in the L-to-M reaction to D85 and D85 remains protonated until BR recovery, another group, termed XH, must be involved in the proton-release mechanism (*14*). Likely candidates in the putative proton-release pathway are R82 and E204 (*4*, *5*). Several investigations are focused on these two groups (*23*−*32*). Recently, R82 was excluded from consideration as the proton-release group (*28*). On the other hand, electrostatic calculations point to a possible upshift of the pK_a of E204 within the protein, and this presents the possibility that it may be protonated in the ground state (*29*). Indeed, exchange of the carboxyl group by the E204Q mutation alters the proton-release kinetics, while the exchange from glutamate to aspartate restores the wild-type (WT) behavior (*1*). Further support for its role as XH has been presented in static BR−M FT-IR difference spectra of E204Q- and E204D-mutated bR. They seem to indicate that carbonyl bands disappear in BR−M difference spectra of the WT and E204D. This was interpreted as the deprotonation of E204 or D204 in M, respectively (*1*). On the basis of these results, several authors propose that E204 represents the proton release group XH (*1*, *30*−*32*).

Here we present time-resolved room-temperature step-scan FT-IR studies with a time resolution of up to 30 ns of the entire photocycles of WT, E204Q, and E204D. These studies of the complete photocycle point to different explanations for the spectral changes between WT and E204X-mutated

†This work was supported by the Deutsche Forschungsgemeinschaft, SFB 394-C2.

* Corresponding author. Phone: ++49-234-700-4461. Fax: ++49-234-709-4238.

[1] Abbreviations: bR, bacteriorhodopsin; BR, light-adapted ground state; WT, wild type; FT-IR, Fourier transform infrared; residues (e.g., E204) are designated using the one-letter code for amino acids. Mutant pigments are designated, e.g., E204Q, where the first letter and the number represents the wild-type residue and the second letter represents the substituted residue.

S0006-2960(97)01701-7 CCC: $15.00
Published on Web 03/19/1998

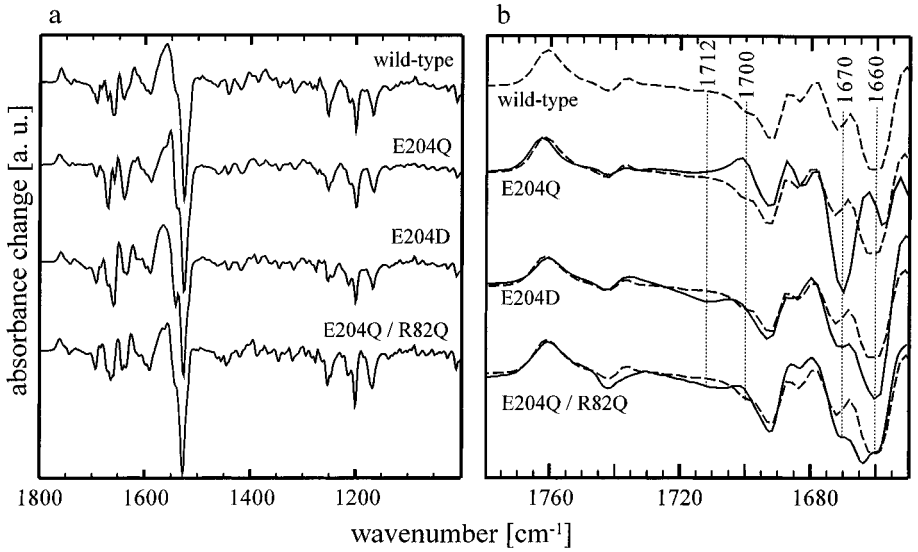

FIGURE 1: Comparison of BR−M low-temperature FT-IR difference spectra (1.5-cm^{-1} resolution) of the WT and E204Q-, E204D-, and E204Q/R82Q-mutated bR. The carbonyl region of the spectra shown in a is enlarged in b, where the dotted lines represent the WT. Conditions: WT (225 K, pH 8, without KCl), E204Q (222 K, pH 7, without KCl), E204D (223 K, pH 7, 1 M KCl), E204Q/R82Q (235 K, pH 7, 1 M KCl). Slightly different conditions are used to obtain most pure BR−M difference spectra of the different proteins.

bR observed in the low-temperature BR−M difference spectra. It is shown that the IR data give no experimental evidence for the deprotonation of E204 or D204 in the L-to-M transition. Our results indicate instead that a complex, H-bonded network is involved in the translocation of a proton to the extracellular surface of bacteriorhodopsin.

MATERIALS AND METHODS

Mutagenesis and Mutant Expression. The site-specific mutants E204D, E204Q, and R82Q/E204Q of bR were prepared as described in ref 33 using the shuttle plasmid pEF191. Mutagenesis was followed by transformation and homologous expression in *H. salinarium* strain MPK40 (*34*). The WT and mutagenized proteins were isolated as purple membrane sheets according to ref 35. The mutations were confirmed from *H. salinarium* transformants by sequencing the *bop* gene fragments amplified by PCR using genomic DNA as the template.

Sample Preparation. Purple membrane sheets were suspended (200 μg in 1 M KCl and 50 mM Tris−HCl buffer) and then centrifuged for 2 h at 200000g to concentrate the sample into a pellet. The pellet was squeezed between two CaF_2 windows separated by a 4 μm Mylar spacer.

The BR−M steady-state spectra in Figure 1 were recorded on a Bruker IFS66 FT-IR spectrometer equipped with a cryostat (Oxford DN704). The samples were light-adapted at 285 K and then cooled to 225 K. The low-temperature difference spectra were measured with 1.5-cm^{-1} spectral resolution by averaging 200 interferograms before and after illumination of the sample by the light of a 100-W halogen lamp, which passes through a Schott KG2 and OG515 filter.

Time-resolved step-scan FT-IR measurements (*36*) were performed on a Bruker IFS66v spectrometer as described previously (*37*). Spectra were recorded with up to 30-ns time resolution and a spectral resolution of 3.5 cm^{-1} between 950 and 1950 cm^{-1}. The bR samples were excited by an excimer-pumped dye laser system at 540 nm (Lambda Physik LPX240i, FL105).

An aim of this work is the determination of the very small and spectrally broad continuum absorbance changes during the photocycle. A nonlinear response of the detector−preamplifier system causes an artifactual time course of the baseline in the difference spectra, which interferes with the broad continuum absorbance (*37*). Therefore, we used a photovoltaic HgCdTe detector (Kollmar Technologies KVMP11-1-J2), which provides a linear behavior between the output signal and the IR intensity in contrast to a photoconductive HgCdTe detector. This is important for very small absorbance changes. In addition, the heating of the sample due to laser excitation does not affect the continuum absorbance under our conditions.

Time-resolved UV−vis spectroscopy is performed with 15-ns time resolution as described previously in ref 37.

Global Fit Analysis. The absorbance changes (ΔA) in the whole infrared spectral region at the wavenumbers ν_i are analyzed with the sums of the n_r exponentials with apparent time constants τ_n and amplitudes a_n, where $\{\tau_n\}$ is the same for all i:

$$\Delta A(\nu_i,t) = \sum_{n=1}^{n_r} a_n(\nu_i)\mathrm{e}^{-t/\tau_n}$$

A detailed description is found in ref 9.

The pH indicator fluorescein (Fluorescein-5-isothiocyanate, Molecular Probes) is covalently linked to K129 at the extracellular surface of bR as described in ref 19. The absorbance changes of fluorescein are obtained at 490 nm by subtraction of the traces of labeled and unlabeled bR under the same salt and pH conditions.

RESULTS

Figure 1 shows static low-temperature, so-called BR−M difference spectra of the WT and the E204Q-, E204D-, and E204Q/R82Q-mutated bR. All four proteins show the typical features of BR−M difference spectra, especially in the fingerprint region between 1300 and 1100 cm^{-1} in Figure

1a. In the enlarged carbonyl region in Figure 1b at 1700 cm^{-1}, a negative band is missing in E204Q, as compared to the WT. This band appears to be upshifted to 1712 cm^{-1} in E204D-mutated bR. According to these observations, the band at 1700 cm^{-1} has been assigned to the carbonyl vibration of E204 and the band at 1712 cm^{-1} to the carbonyl vibration of D204 (*1*).

Besides these spectral changes, additional spectral features appear in E204Q at 1670 and 1660 cm^{-1} in a spectral region, that was not presented in ref 1. These additional features indicate that not only do spectral changes appear in the E204Q mutant due to the disappearance of E204 carbonyl vibrations but also other protein groups change their spectral behavior due to the mutation. Therefore, the former given assignment (*1*) is not unequivocal because other groups could also cause the band at 1700 cm^{-1}.

Nevertheless, the BR−M difference spectrum of the E204D mutant shows a better overall agreement to the WT difference spectrum and seems to allow, at first sight, an assignment of the band at 1712 cm^{-1} to the upshifted carbonyl vibration of D204. But contrary to this assignment are the spectral changes in the difference spectrum of the E204Q/R82Q double-mutated bR. Its difference spectrum shows similar spectral changes as E204D, i.e., missing a negative band at 1700 cm^{-1} and an additional negative band at 1712 cm^{-1}, without a D at position 204.

In summary, the difference spectra in Figure 1 show that the band at 1700 cm^{-1} cannot unequivocally be assigned to E204 and the results on E204Q/R82Q contradict the assignment of the band at 1712 cm^{-1} to D204.

To elaborate all deviations in the spectra induced by the mutation of E204, we used time-resolved step-scan FT-IR spectroscopy with 30-ns time resolution (*37*) to investigate the complete photocycles of the WT, E204Q, and E204D at room temperature. In Figure 2, the absorbance changes of the C−C retinal stretching vibrations at 1186 cm^{-1} are given as an indicator of photocycle kinetics. In WT, its appearance (not time-resolved) reflects the *all-trans*- to 13-*cis*-retinal isomerization. The time constant τ_1 indicates the K-to-L transition, τ_2 and τ_5 indicate the deprotonation of the Schiff base in the L-to-M transition, and τ_4 indicates the reprotonation of the Schiff base in the M-to-N transition. The final disappearance of absorption by τ_3 and τ_6 marks the relaxation to the *all-trans* bR ground state (*9*).

In E204Q-mutated bR (Figure 2c!), the overall photocycle is slowed (note the different time scales). The appearance of M is faster as compared to WT, and L does not accumulate. The M-to-O transition is slowed, as indicated by the slower reappearance of the band at 1186 cm^{-1}. The concomitant appearance of a band at 1509 cm^{-1} (data not shown) indicates that, in contrast to WT, an O intermediate accumulates without significant amounts of the N intermediate (*16*). Also the final relaxation to the BR ground state is slowed. The deviations from the WT are too large to compare the difference spectra of the WT and E204Q directly with each other.

In the E204D-mutated protein, the photocycle is similar to that of the WT (Figure 2b), but less L and more O accumulate. Interestingly, the N-to-O transition is resolved, which is not the case in WT. The reappearance of the band at 1186 cm^{-1} is described by two time constants (2.2 and 13 ms).

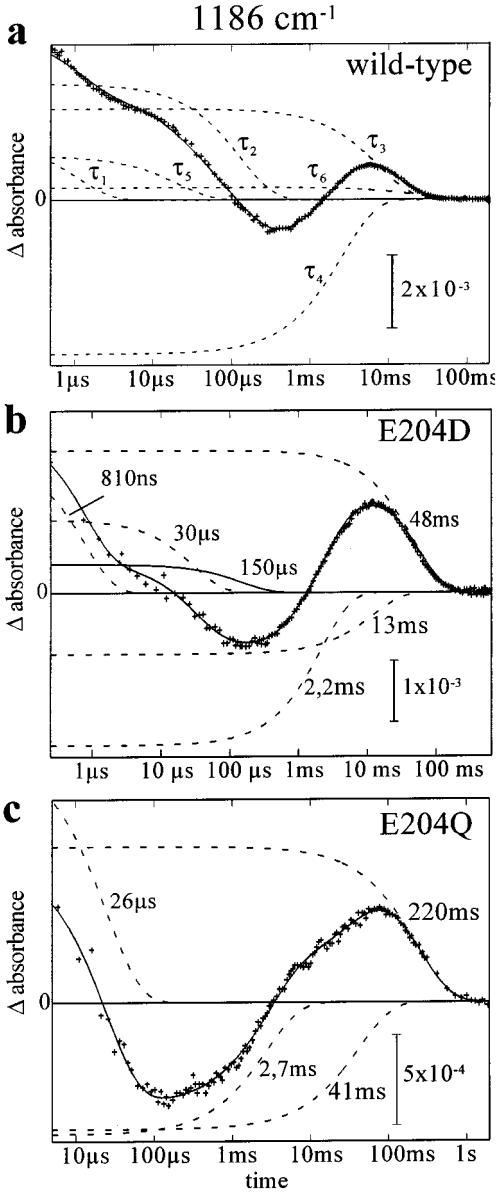

FIGURE 2: Time courses at 1186 cm^{-1} with 30-ns time resolution monitored the photocycle kinetics of the WT and E204D-, and E204Q-mutated bR with multiexponential fit curves as revealed by global fit analysis. The dotted lines are single exponentials, which compose the fitted curve. All measurements were performed at 293 K in 1 M KCl at pH 7.0 (E204D: pH 7.5).

The absorbance changes in the carbonyl region are quantitatively seen in the corresponding amplitude spectra of the WT and E204D in Figure 3. As compared to the difference spectra, the amplitude spectra contain only the absorbance changes of the respective transition. Therefore, amplitude spectra are more useful than the conventional used difference spectra, which represent the absorbance changes between the ground state and the respective intermediate. Difference spectra also contain, in addition to amplitude spectra, absorbance changes that are not due to the respective transition. For example, an absorbance change, which takes place in the BR-to-K transition and remains until M, appears in the BR−M difference spectra but not in the τ_5 and τ_2 amplitude spectra describing only absorbance changes in the L-to-M transition. In contrast to the difference spectra, disappearing bands are positive and appearing bands are negative in the amplitude spectra. For a more detailed

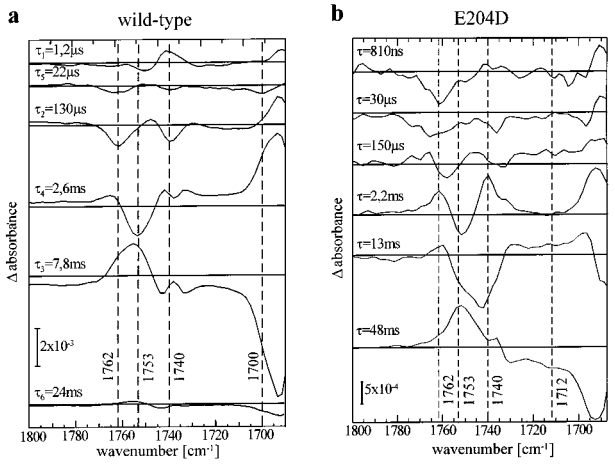

FIGURE 3: Amplitude spectra of the single exponentials in the spectral range between 1690 and 1800 cm^{-1} describing the photocycle reactions of (a) WT and (b) E204D as revealed by global fit analysis. Both photocycles of WT and E204D can be described by a sum of six exponentials. In contrast to difference spectra, appearing bands have negative amplitudes. For example, the band at 1762 cm^{-1} appears with negative bands in the τ_2 and τ_5 amplitude spectra of the WT. Experimental conditions as in Figure 2.

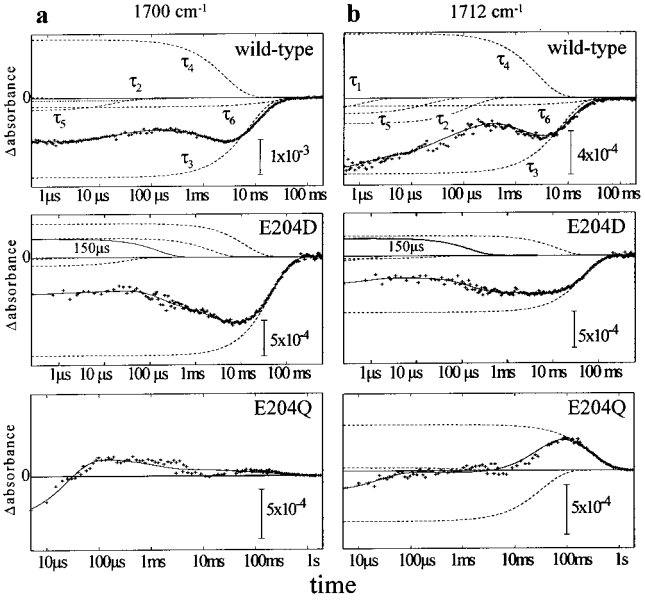

FIGURE 4: Time courses of the WT and E204D-, and E204Q-mutated bR at (a) 1700 and (b) 1712 cm^{-1}. The 150-μs time constant in E204D bR is highlighted. Experimental conditions as in Figure 2.

description of the amplitude spectra of the WT, see ref 9. In the WT, the appearance of the D85 carbonyl vibration at 1762 cm^{-1} (indicating its protonation by a negative band) is seen in the τ_5 and τ_2 amplitude spectra, its downshift to 1753 cm^{-1} in the τ_4 amplitude spectrum (indicating its environmental change in M by a difference band), and its final disappearance in the τ_3 and τ_6 amplitude spectra (indicating its deprotonation in BR by a positive band). Assuming that the negative band at 1700 cm^{-1} is due to E204 and that E204 deprotonates in M, then a positive band, comparable in size to the negative band at 1762 cm^{-1}, should appear at 1700 cm^{-1} in the τ_5 and τ_2 amplitude spectra. Because the appearance of such a band is not observed either in the τ_5 or in the τ_2 amplitude spectra, the data in Figure 1 and ref 1 cannot be used as arguments for the deprotonation of E204 during the L-to-M transition. The band appearing at about 1693 cm^{-1} with contributions at 1700 cm^{-1} in the τ_4 amplitude spectrum is not affected by the mutation (Figure 1) and, therefore, does not represent E204. For comparison, see the amplitude spectra at 2.2 ms of E204D in Figure 3b. However, a deprotonation of XH should take place earlier in the L-to-M reaction but not in the M-to-N reaction, which is described by τ_4.

In the E204D-mutated protein, the kinetics are changed as compared to the WT: the band at 1762 cm^{-1}, indicative of M, appears within 810 ns much faster than in the WT and increases further with a time constant of 30 μs (Figure 3b). It undergoes a downshift to 1753 cm^{-1}, indicative of N and O, within 150 μs, 2.2 ms, and 13 ms, and disappears within 48 ms. The 150-μs time constant has no direct equivalent in the WT. It shows a broad absorbance decrease between 1730 and 1700 cm^{-1}. The amplitude spectrum of the 2.2-ms time constant indicates, better resolved than in the WT, deprotonation of D96 in N at 1740 cm^{-1} and corresponds to τ_4 (*14*). The amplitude spectrum of the 13-ms time constant resolves the N-to-O transition even better than in the WT. It indicates the reprotonation of D96 in O in agreement with the results on the WT (*9*). As compared to 1762 cm^{-1}, at 1712 cm^{-1} no specific band disappears in the different amplitude spectra, which would indicate a transient deprotonation of D204. Instead, a broad absorbance change appears in the M-to-N transition with time constants of 150 μs and 13 ms and disappears within 48 ms. In summary, the absorbance changes in the carbonyl region exclude a deprotonation of D204 and most likely of E204 during M's appearance.

But how can one explain the spectral changes in the carbonyl region between the WT and the mutants as discussed for Figure 1? One possibility arises by comparison of the absorbance changes at 1700 and 1712 cm^{-1}, as shown in Figure 4. All three proteins exhibit an instantaneous, not time-resolved, absorbance disappearance at 1700 cm^{-1}. The time courses of the WT and the mutant E204D deviate slightly at 1700 cm^{-1}. The WT absorbance remains nearly constant during M formation in the first 500 μs and does not decrease, as would be expected for a deprotonation of E204. Therefore, the time course of the absorbance changes of the WT at 1700 cm^{-1} gives no indication of a disappearing carbonyl vibration in the L-to-M transition. The absorbance of E204D disappears at 1700 cm^{-1} after M formation with a time constant of 150 μs. The 150-μs time constant describes a broad absorbance decrease between 1700 and 1730 cm^{-1}, as can be seen in the amplitude spectra in Figure 3b.

In the WT, the absorbance at 1712 cm^{-1} increases during M formation. In contrast, in E204D, the time course at 1712 cm^{-1} does not change with the two time constants of 810 ns and 30 μs, which mainly describe M formation. The time course of the absorbance changes of E204D at 1712 cm^{-1} gives no indication for a disappearing D204 carbonyl vibration in the K/L-to-M transition. Further, the absorbance decreases with the 150-μs time constant, which describes the broad absorbance decrease between 1700 and 1730 cm^{-1}. This absorbance decrease at 1712 cm^{-1}, in addition to a negative band at 1712 cm^{-1} that occurs already in the BR−K difference spectra (data not shown) and remains until M, gives the false appearance of a negative band at 1712 cm^{-1}

in the static BR−M difference spectra of E204D (Figure 1b). The difference spectra presented in Figure 1 also contain, in contrast to amplitude spectra, absorbance changes that appear in K and remain up to M. Furthermore, at 225 K and steady-state illumination, not only pure M but also some amount of other preceding and following intermediates accumulate, and therefore, the 150-μs rate may also contribute to the BR−M spectra of E204D.

In E204Q (bottom in Figure 4), the absorbance changes at 1700 and 1712 cm^{-1} are completely different than in the WT. Due to this different kinetics, a negative band seems to disappear in the BR−M difference spectrum at 1700 cm^{-1} in Figure 1. But this band does not disappear due to the absence of the carboxyl group of E204. Rather, the time-resolved data now show that this is due to the different photocycle kinetics of the WT and of E204Q. Therefore, their difference spectra cannot simply be compared to each other for band assignment.

If we now exclude the deprotonation of E204 in M, the questions arise, why does the mutation E204Q influence the proton-release kinetics and why is the proton-release kinetics of the WT restored in E204D-mutated bR?

For an answer, we consider the continuum absorbance change in Figure 5. The continuum absorbance change is unperturbed between 1850 and 1800 cm^{-1} because there are no specific bands in this spectral region. Continuum absorbance changes can be used to monitor the polarizability changes of a delocalized proton within an H-bonded network (*38*). The continuum absorbance changes presented in Figure 5 are analyzed together with all absorbance changes between 1000 and 1900 cm^{-1} by a global fit procedure. In the WT at pH 7, the continuum band decrease can be described by the characteristic time constant τ_2 and to a much smaller amount by τ_5. It decreases further in the M-to-N reaction with the time constant τ_4. The further continuum absorbance decrease in the M-to-N transition is proposed to indicate a proton transfer between D96 and the Schiff base via an intramolecular H-bonded network (*39*). The continuum absorbance kinetics deviate relative to the baseline as compared with the earlier published kinetics (*39*). This derives from the small nonlinearities of the photoconductive HgCdTe detectors used in the former experiments instead of the current photovoltaic detector (*37*). These nonlinearities lead to a time-dependent baseline shift in the difference spectra. In E204Q-mutated bR, no continuum absorbance change is observed at all. This proves in addition that artifacts due to possible heating of the sample by the laser pulse do not cause broad absorbance changes under our measuring conditions. It shows, furthermore, that proton release into the bulk water also does not contribute significantly to the continuum absorbance change under our measuring conditions because the proton uptake from the bulk, which occurs during the M decay, and the proton release into the bulk, which occurs in the O-to-BR transition, do not influence the continuum absorbance. A further decrease of the continuum absorbance in the M-to-N transition is not seen because in the E204Q mutant, the N intermediate does not accumulate. In E204D-mutated bR, in which the proton-release kinetics is restored, the continuum absorbance change reappears as in the WT protein at pH 7.

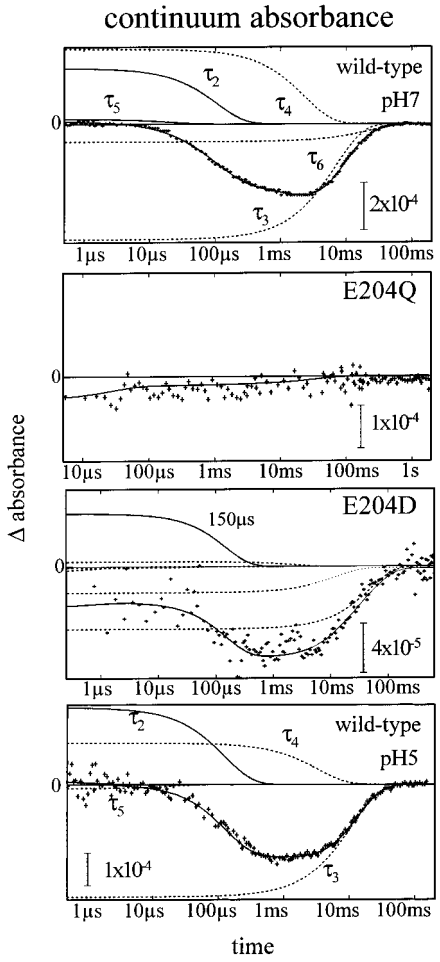

FIGURE 5: Time courses of the broad continuum absorbance averaged between 1800 and 1850 cm^{-1} for WT at pH 7, E204D at pH 7.5, E204Q at pH 7, and WT at pH 5. The experiments are all performed at 293 K and 1 M KCl. The time courses are analyzed by a global fit procedure, which considers all IR absorbance changes between 1000 and 1900 cm^{-1}. The following time constants are calculated: WT pH 7 (τ_1 = 1.2 μs, τ_5 = 22 μs, τ_2 = 130 μs, τ_4 = 2.6 ms, τ_3 = 7.8 ms, τ_6 = 24 ms), E204Q (τ_b = 26 μs, τ_c = 1.2 ms, τ_d = 35 ms, τ_e = 320 ms), E204D (τ_a = 810 ns, τ_b = 30 μs, τ_c = 150 μs, τ_d = 2.2 ms, τ_e = 13 ms, τ_f = 48 ms), WT pH 5 (τ_1 = 1.3 μs, τ_5 = 22 μs, τ_2 = 128 μs, τ_4 = 3.5 ms, τ_3 = 11 ms).

Assuming an H-bonded network represents the group that releases the proton into the bulk, then the continuum absorbance should not decrease in the L-to-M transition at a pH below the pK_a of this group. Below pH 5.8, the proton release into the bulk is delayed and takes place during BR recovery (*22*). Surprisingly, in the WT at pH 5, the continuum absorbance change is not altered as compared to pH 7. The absorbance decrease is still described by the time constants τ_2 and τ_4. The amplitudes of the continuum absorbance change at pH 7 and 5 are the same when normalized to the 1527-cm^{-1} band. Therefore, the process, which is described by the continuum absorbance change, does not have a pK_a of 5.8, and the continuum absorbance change cannot indicate the proton release into the bulk.

In Figure 6, the appearance of a proton at the extracellular surface and the continuum absorbance change (same data as in Figure 5) are compared. The appearance of the proton is measured by the pH-indicator dye fluorescein, which is covalently bound to K129 at the extracellular surface of bR. Now, both absorbance changes are analyzed separately

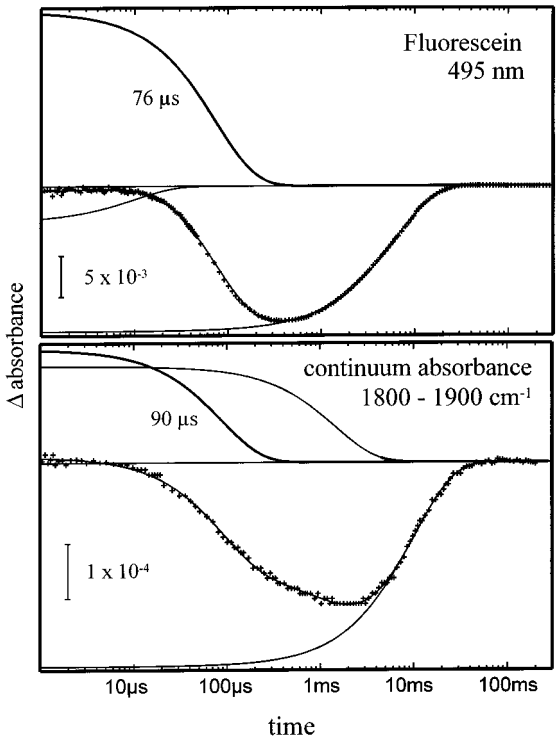

FIGURE 6: Comparison of the time course of the appearance of the proton at the extracellular surface of bR measured by convalently bound fluorescein and the IR continuum absorbance, which is averaged between 1800 and 1900 cm^{-1}. The time courses are not analyzed with the global fit procedure but alone. The continuum absorbance is measured at 293 K, 1 M KCl, and 50 mM Tris, pH 7.0. The fluorescein signal is measured in a 10 μM bR suspension at 295 K, 100 mM KCl, pH 7.4, and without buffer.

without considering absorbance changes at other wavenumbers, which represent the photocycle kinetics. The fluorescein absorbance decreases with a time constant of 76 μs. This indicates the appearance of a proton at the protein surface, in agreement with refs 19 and 20. There is a small contribution of a 10-μs time constant. However, we cannot exclude that this is due to a small influence of the bound fluorescein on the photocycle, which would cause an artifact in the subtraction. If the continuum absorbance is analyzed separately from the other IR absorbance changes, then its disappearance can be described by a single exponential similar to the fluorescein absorbance change. The residual plots of the two different fits of the continuum absorbance in Figures 5 and 6 are almost identical. Therefore, it cannot be distinguished if the continuum absorbance disappears with the rates describing the L-to-M transition or the apparent rate that describes the appearance of the proton at the surface. The small deviation between the two apparent time constants (90 μs vs 76 μs) seems to be caused by slightly different pH and temperature conditions. The IR experiments are performed in thin films, whereas the fluorescein measurements are performed in suspension.

In Figure 7, time-resolved BR−M difference spectra at pH 5 and 7 are compared. The spectra, which are taken 500 μs after laser excitation, show the typical features of the BR−M spectra. The fingerprint region between 1300 and 1100 cm^{-1} shows a deprotonated Schiff base. The proton acceptor D85 is protonated at pH 7, indicated by the positive carbonyl band at 1761 cm^{-1} (enlarged part of Figure 7). At pH 5, this band shifts to 1763 cm^{-1}, which indicates

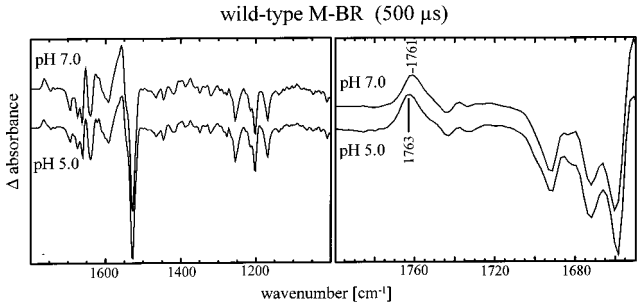

FIGURE 7: Comparison of time-resolved BR−M FT-IR difference spectra, which are taken 500 μs after laser excitation at pH 7 and 5. Experimental conditions: 293 K, 1 M KCl.

a slightly more hydrophobic environment of D85. Apart from this difference, the two spectra are almost identical, especially in the carbonyl region above 1700 cm^{-1}. A deviation at 1700 cm^{-1} would be expected for a deprotonation of E204 (*1*). This gives further indication that E204 does not represent XH.

DISCUSSION

Based on the results of static FT-IR experiments, it was proposed earlier that the proton-release group called XH is E204 (*1*). The negative bands at 1700 and 1712 cm^{-1} in the BR−M difference spectra have been interpreted as the disappearing carbonyl vibrations of E204 and D204, respectively.

The results presented here show that the E204Q mutation induces large deviations in the photocycle as compared to the WT. Therefore, the BR−M difference spectra of E204Q and of the WT cannot simply be compared to each other for band assignments. Furthermore, the amplitude spectra of the WT do not show a distinct disappearing band at 1700 cm^{-1} in the L-to-M transition, which would be expected if E204 would deprotonate. The photocycles of the WT and E204D-mutated bR are more similar to each other, and therefore, the arguments in ref 1 place more stress on this mutant. Nevertheless, the results presented above negate the possibility that the band at 1712 cm^{-1} is caused by D204 because the same features seen in E204D-mutated bR are also observed in E204Q/R82Q double mutated bR, which lacks a carboxyl group at position 204. The spectral deviations between the WT and E204D observed in the low-temperature BR−M difference spectra are caused by an absorbance change at 1712 cm^{-1}, which appears in K and remains up to M. Furthermore, small deviations in their photocycle kinetics also seem to contribute. These results show that the data given in ref 1 cannot be used as arguments for a deprotonation of D204 in the L-to-M transition. In summary, there is no experimental evidence from the FT-IR data for deprotonation of E204 or D204 in the L-to-M transition. It is very unlikely that the deprotonation of E204 would not be reflected in the IR spectra. Conclusively, E204 does not seem to represent the proton-release group XH.

On the other hand, the E204Q mutation disturbs the proton-release kinetics (*1*). In this mutant, proton uptake precedes proton release, contrary to the WT-release kinetics. Thus, E204 seems to be involved in the proton-release mechanism. An alternative explanation of the results would be that, instead of being the group XH itself, E204 could be part of a highly coupled H-bonded network, which is

involved in the proton-release mechanism. A proton might be delocalized within this network. In this case, the negatively charged E204 would be a stabilizing part of such a network, but it would not represent the protonated group XH itself.

There is accumulating experimental evidence for H-bonded networks in bR. Different biophysical techniques provide a model in which the negatively charged counterion of the positively charged Schiff base does not seem to be a single residue but rather a complex hydrogen-bonded network spanning from the Schiff base to the extracellular surface of bR. It contains D85, D212, Y185, Y57, R82, E204, and a few firmly bound water molecules (*40*−*44*). Neutron scattering experiments show bound water molecules in a top view below and above the Schiff base region (*45*), in agreement with resonance Raman experiments (*46*). Four of the water molecules are firmly bound and resist extraction even under vacuum (*45*). Further evidence for bound internal water molecules undergoing H-bond changes during the photocycle is provided by FT-IR experiments (*47*, *48*). Also, electron microscopy studies point to internal water molecules. In these studies, three cavities between D85, R82, and E204 are proposed. Each possibly contains a water molecule (*5*). Energy minimized molecular dynamics calculations based on this structural model propose a string of water molecules from D85 via R82 and E204 (*49*, *50*). Such a string of water molecules could represent a large part of a hydrogen-bonded network. Further, carboxyl groups such as E9, E74, and E194 are located in a cluster at the extracellular surface (*5*, *51*) and could also contribute. Nevertheless, one has to consider that the structural resolution is about 3.5 Å horizontal and about 5 Å vertical to the membrane plane. This causes some uncertainties in the exact positioning of the side groups and bound water molecules in the proposed model (*5*, *52*).

The polarizability of a delocalized proton in an H-bonded network causes a spectrally broad continuum absorbance (*38*). In the WT at pH 7, such continuum absorbance disappears in the L-to-M transition and shows a further decrease in the M-to-N transition (Figure 5). The further decrease in the M-to-N transition is assigned to the proton transfer via an H-bonded network from D96 to the Schiff base (*39*). In a global fit analysis, which considers all IR absorbance changes between 1000 and 1900 cm^{-1}, the disappearance of the continuum absorbance can be described by the time constant $\tau_2 = 130$ μs, and with a much smaller amplitude, $\tau_5 = 20$ μs (Figure 5) of the L-to-M transition. But it is also possible to describe this disappearance when analyzed separately with only one exponential, which has the same time constant as the appearance of a proton at the extracellular surface of bR (Figure 6). When E204 is mutated to Q, the continuum absorbance change in the L-to-M transition is no longer observed. The transfer of the proton to the surface as measured with fluorescein (data not shown) and the release are delayed from the L-to-M transition to the O-to-BR transition. In E204D, the WT proton-release kinetics is restored again, and the continuum absorbance changes again show the same time dependence as in the WT at pH 7. For these reasons, we conclude that an intramolecular H-bonded network is involved in the mechanism that leads to the appearance of a proton at the extracellular surface. E204 seems to stabilize this network, and the removal of the protonable carboxyl group in E204Q disturbs this complex, well-balanced network. It is proposed that in E204Q, the proton is released from D85 when it becomes deprotonated in the O-to-BR back-reaction.

Zimányi et al. have shown that the release of a proton into the bulk medium has a pK_a of 5.8 (*22*). By comparing time-resolved FT-IR measurements above and below pH 5.8, it is possible to distinguish whether the continuum aborbance change is directly coupled to the release of a proton into the bulk or represents another step in the release mechanism. Our measurements show the same time dependence of the continuum absorbance change at pH 5 and 7, although at pH 5, the release of the proton into the bulk is delayed until the O-to-BR transition. Therefore, the H-bonded network that causes the continuum absorbance change cannot be the terminal proton-release group itself. The proton is not directly released from the network into the bulk.

At pH 7, the proton appears at the surface with a time constant of about 80 μs. There are not yet pH indicators available with a pK_a near 5.8, which can be bound covalently to the protein. Therefore, the time course of the appearance of the proton at the surface of bR is not resolved below pH 5.8. From our data, it seems that the proton-transfer mechanism to the surface is the same at pH 5 and 7 because the continuum absorbance change is not altered between pH 7 and 5. Only the release from the surface to the bulk medium seems to differ within this pH range. However, this has to be proven in further studies with covalently bound pH indicators, which have a pK_a below 5.8.

Consitent with this conclusion are the WT BR−M difference spectra taken 500 μs after light excitation at pH 5 and 7 (Figure 7). These spectra do not show obvious deviations, which could indicate a different protonation state of a single residue or the H-bonded network between pH 5 and 7. Balashov et al. predict a group X′H, which should have a pK_a of 9.7 in the BR ground state and a pK_a of 4.8 when D85 becomes protonated in the blue membrane (*25*, *53*). X′H is proposed to be identical with the proton-release group XH and should have a pK_a of 5.8 in the M intermediate. In contrast, the BR−M difference spectra give no indication for a different protonation state of X′H in the M intermediate between pH 5 and 7. Nevertheless, X′H could be represented by the H-bonded network. But in this case, the pK_a of X′H has to be below 5 in the M intermediate.

Three glutamates (E9, E74, and E194) are located in a cluster at the surface of bR and could form a protonable network, which may release the proton into the bulk about 1 ms after light excitation of bR. But unfortunately, the time scale of this process overlaps with the proton-uptake reaction and the reprotonation of the Schiff base. Therefore, more detailed investigations of the pH dependence of the continuum absorbance in this time range are necessary to determine the release process from the surface of the protein into the bulk.

Experimental evidence for proton transfer via an intramolecular H-bonded network on the proton-release pathway is also given by the kinetic isotope effect in D_2O (*54*). The time constant τ_2 mainly describing the deprotonation of the Schiff base and protonation of D85 in the L-to-M transition is slowed by a factor of 6 in D_2O (*54*). This is the typical kinetic effect expected for proton transfer via a highly ordered ice-like H-bonded network (*54*). In addition, the proton-

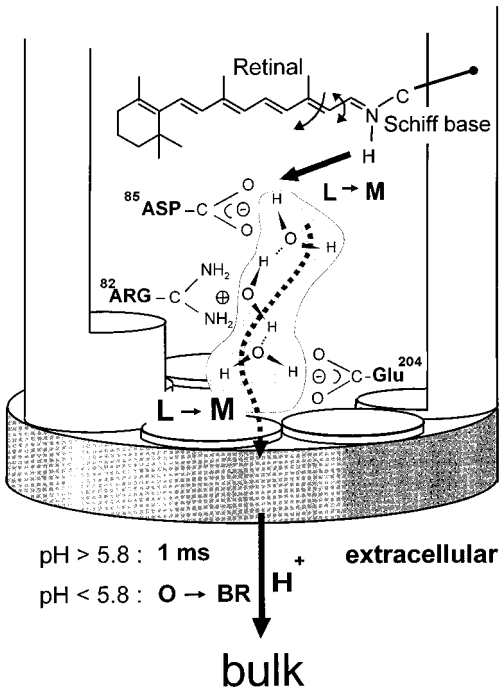

FIGURE 8: Postulated model of the retinal binding site and the extracellular half of the proton-release channel. The *all-trans*- to 13-*cis*-retinal isomerization results in a proton transfer from the Schiff base to D85 in the L-to-M transition. In the same transition, an H-bonded network releases a proton to the extracellular surface of bR. The proton release into the bulk medium is pH-dependent. At pH 7, the proton leaves the surface after 1 ms, whereas at pH 5, it remains at the surface until the O-to-BR transition.

release kinetics in the L-to-M transition is slowed by the same factor (*17*, *55*). Furthermore, studies of the pH-dependent protonation changes during bacteriorhodopsin's reconstitution from apoprotein and retinal also point to a hydrogen-bonded network in the proton release pathway, which has the capacity to bind two protons (*56*).

The conclusions are summarized in a model presented in Figure 8. The *all-trans*- to 13-*cis*-retinal isomerization results in a pK_a decrease of the Schiff base and a pK_a increase of D85. This enables the proton transfer from the Schiff base to D85 in the L-to-M transition. Due to the protonation of D85, a proton is released to the extracellular surface by an H-bonded network, which is stabilized by several residues including R82 and E204. Internal bound water molecules and further not yet identified groups also seem to contribute to the network. At pH > 5.8, about 1 ms after the proton of the network appears at the surface, a proton is released into the bulk medium (*19*, *20*, *22*, *57*). At pH < 5.8, D85 seems to have to reprotonate the H-bonded network until a proton is released from the surface into the bulk. The proton transfer from the highly ordered, ice-like, H-bonded network to the less ordered surface increases the entropy and seems to make a back-reaction of the pumped proton back into the protein unlikely. This entropy increase may contribute to the unidirectionality of the pump and, therefore, to the reprotonation switch.

After submitting this paper, (i) a substantially improved bR structure was published, which shows, in agreement with our proposal, bound internal water molecules between D85 and the surface, supporting the existence of an H-bonded network (*58*); (ii) a recently published electron microscopy study also points to a deprotonated E204 in the BR ground state, in agreement with the presented results (*59*).

ACKNOWLEDGMENT

We are very grateful to Dr. M. P. Krebs for providing us with the *H. salinarium* strain MPK40 and especially to Dr. D. Oesterhelt for making the shuttle plasmid and the transformation instructions available. We appreciate very much the dedicated work on bR mutageneses of Axel Hartz and the relevant information and stimulating discussions with Dr. Volker Hildebrandt. We also thank Dr. David Rumschitzki for his help in English-style corrections.

REFERENCES

1. Brown, L. S., Sasaki, J., Kandori, H., Maeda, A., Needleman, R., and Lanyi, J. K. (1995) *J. Biol. Chem. 270*, 27122−27126.
2. Oesterhelt, D., and Stoeckenius, W. (1971) *Nature New Biol. 233*, 149−152.
3. Oesterhelt, D., Tittor, J., and Bamberg, E. (1992) *J. Bioenerg. Biomembr. 24*, 181−191.
4. Henderson, R., Baldwin, J. M., Ceska, T. A., Zemlin, F., Beckmann, E., and Downing, K. H. (1990) *J. Mol. Biol. 213*, 899−929.
5. Grigorieff, N., Ceska, T. A., Downing, K. H., Baldwin, J. M., and Henderson, R. (1996) *J. Mol. Biol. 259*, 393−421.
6. Lozier, R. H., Bogomolni, R. A., and Stoeckenius, W. (1975) *Biophys. J. 15*, 955−963.
7. Xie, A. H., Nagle, J. F., and Lozier, R. H. (1987) *Biophys. J. 51*, 627−635.
8. Ames, J. B., and Mathies, R. A. (1990) *Biochemistry 29*, 7181−7190.
9. Hessling, B., Souvignier, G., and Gerwert, K. (1993) *Biophys. J. 65*, 1929−1941.
10. Braiman, M., and Mathies, R. (1982) *Proc. Natl. Acad. Sci. U.S.A. 79*, 403−407.
11. Engelhard, M., Gerwert, K., Hess, B., Kreutz, W., and Siebert, F. (1985) *Biochemistry 24*, 400−407.
12. Braiman, M. S., Mogi, T., Marti, T., Stern, L. J., Khorana, H. G., and Rothschild, K. J. (1988) *Proteins: Struct., Funct., Genet. 3*, 219−229.
13. Gerwert, K., Hess, B., Soppa, J., and Oesterhelt, D. (1989) *Proc. Natl. Acad. Sci. U.S.A. 86*, 4943−4947.
14. Gerwert, K., Souvignier, G., and Hess, B. (1990) *Proc. Natl. Acad. Sci. U.S.A.*, 87, 9774−9778.
15. Fahmy, K., Weidlich, O., Engelhard, M., Tittor, J., Oesterhelt, D., and Siebert, F. (1992) *Photochem. Photobiol. 56*, 1073−1083.
16. Smith, S. O., Pardeon, J., Mulder, P. P., Curry, B., Lugtenburg, J., and Mathies, R. A. (1983) *Biochemistry 22*, 6141−6148.
17. Heberle, J., and Dencher, N. A. (1990) *FEBS Lett. 277*, 277−280.
18. Cao, Y., Brown, L. S., Needleman, R., and Lanyi, J. K. (1993) *Biochemistry 32*, 10239−10248.
19. Heberle, J., and Dencher, N. A. (1992) *Proc. Natl. Acad. Sci. U.S.A. 89*, 5996−6000.
20. Alexiev, U., Mollaaghababa, R., Scherrer, P., Khorana, H. G., and Heyn, M. P. (1995) *Proc. Natl. Acad. Sci. U.S.A. 92*, 372−376.
21. Váró, G., and Lanyi, J. K. (1990) *Biochemistry 29*, 6858−6865.
22. Zimányi, L., Váró, G., Chang, M., Ni, B., Needleman, R., and Lanyi, J. K. (1992) *Biochemistry 31*, 8535−8543
23. Otto, H., Marti, T., Holz, M., Mogi, T., Stern, L. J., Engel, F., Khorana, H. G., and Heyn, M. P. (1990) *Proc. Natl. Acad. Sci. U.S.A. 87*, 1018−1022.
24. Balashov, S. P., Govindjee, R., Kono, M., Imasheva, E., Lukashev, E., Ebrey, T. G., Crouch, R. K., Menick, D. R., and Feng, Y. (1993) *Biochemistry 32*, 10331−10343.
25. Balashov, S. P., Govindjee, R., Imasheva, E. S., Misra, S., Ebrey, T. G., Feng, Y., Crouch, R. K., and Menick, D. R. (1995) *Biochemistry 34*, 8820−8834.

26. Kandori, H., Yamazaki, Y., Hatanaka, M., Needleman, R., Brown, L. S., Richter, H.-T., Lanyi, J. K., and Maeda, A. (1997) *Biochemistry 36*, 5134−5141.
27. Misra, S., Govindjee, R., Ebrey, T. G., Chen, N., Ma, J.-X., and Crouch, R. K. (1997) *Biochemistry 36*, 4875−4883.
28. Govindjee, R., Misra, S., Balashov, S. P., Ebrey, T. G., Crouch, R. K., and Menick, D. R. (1996) *Biophys. J. 71* (2), 1011−1023.
29. Scharnagl, C., Hettenkofer, J., and Fischer, S. F. (1995) *J. Phys. Chem. 99*, 7787−7800.
30. Richter, H. T., Brown, L. S., Needleman, R., and Lanyi, J. K. (1996) *Biochemistry 35*, 4054−4062.
31. Richter, H. T., Needleman, R., and Lanyi, J. K. (1996) *Biophys. J. 71*, 3392−3398.
32. Brown, L. S., Needleman, R., and Lanyi, J. K. (1996) *Biochemistry 35*, 16048−16054.
33. Ferrando, E., Schweiger, U., and Oesterhelt, D. (1993) *Gene 125*, 41−47.
34. Krebs, M. P., Hauss, T., Heyn, M. P., RajBhandary, U. L., and Khorana, H. G. (1991) *Proc. Natl. Acad. Sci. U.S.A. 88*, 859−863.
35. Oesterhelt, D., and Stoeckenius, W. (1974) *Methods Enzymol. 31*, 667−678.
36. Uhmann, W., Becker, A., Taran, C., and Siebert, F. (1991) *Appl. Spectrosc. 45*, 390−397.
37. Rammelsberg, R., Hessling, B., Chorongiewski, H., and Gerwert, K. (1997) *Appl. Spectrosc. 51*, 558−562.
38. Zundel, G. (1992) *Trends Phys. Chem. 3*, 129−156.
39. le Coutre, J., Tittor, J., Oesterhelt, D., and Gerwert, K. (1995) *Proc. Natl. Acad. Sci. U.S.A. 92*, 4962−4966.
40. Rath, P., Krebs, M. P., He, Y., Khorana, H. G., and Rothschild, K. J. (1993) *Biochemistry 32*, 2272−2281.
41. Sonar, S., Marti, T., Rath, P., Fischer, W., Coleman, M., Nilsson, A., Khorana, H. G., and Rothschild, K. J. (1994) *J. Biol. Chem. 269*, 28851−28858.
42. Fischer, W. B., Sonar, S., Marti, T., Khorana, H. G., and Rothschild, K. J. (1994) *Biochemistry 33*, 12757−12762.
43. Govindjee, R., Kono, M., Balashov, S. P., Imasheva, E., Sheves, M., and Ebrey, T. G. (1995) *Biochemistry 34*, 4828−4838.
44. Hatanaka, M., Sasaki, J., Kandori, H., Ebrey, T. G., Needlemann, R., Lanyi, J. K., and Maeda, A. (1996) *Biochemistry 35*, 6308−6312.
45. Papadopoulos, G., Dencher, N. A., Zaccai, G., and Büldt, G. (1990) *J. Mol. Biol. 214*, 15−19.
46. Hildebrandt, P., and Stockburger, M. (1984) *Biochemistry 23*, 5539−5548.
47. Maeda, A., Sasaki, J., Shichida, Y., and Yoshizawa, T. (1992) *Biochemistry 31*, 462−467.
48. Yamazaki, Y., Satoru, T., Hazime, S., Kandori, H., Needleman, R., Lanyi, J. K., and Maeda, A. (1996) *Biochemistry 35*, 4063−4068.
49. Humphrey, W., Logunov, I., Schulten, K., and Sheves, M. (1994) *Biochemistry 33*, 3668−3678.
50. Engels, M., Gerwert, K., and Bashford, D. (1995) *Biophys. Chem. 56*, 95−104.
51. Balashov, S. P., Imasheva, E. S., Ebrey, T. G., Chen, N., Menick, D. R., and Crouch, R. K. (1997) *Biochemistry 33*, 8671−8676.
52. Bashford, D., and Gerwert, K. (1992) *J. Mol. Biol. 224*, 473−486.
53. Balashov, S. P., Imasheva, E. S., Govindjee, R., and Ebrey, T. G. (1996) *Biophys. J. 70*, 473−481.
54. Le Coutre, J., and Gerwert, K. (1996) *FEBS Lett. 398*, 333−336.
55. Cao, Y., Brown, L. S., Sasaki, J., Maeda, A., Needleman, R., and Lanyi, J. K. (1995) *Biophys. J. 68*, 1518−1530.
56. Rüdiger, M., Tittor, J., Gerwert, K., and Oesterhelt, D. (1997) *Biochemistry 36*, 4867−4874.
57. Heberle, J., Riesle, J., Thiedemann, G., Oesterhelt, D., and Dencher, N. A. (1994) *Nature 370*, 379−382.
58. Pebay-Peyroula, E., Rummel, G., Rosenbusch, J. P., and Landau, E. M. (1997) *Science 77*, 1676−1681.
59. Kimura, Y., Vassylyev, D. G., Miyazawa, A., Kidera, A., Matsushima, M., Mitsuoka, K., Murata, K., Hirai, T., and Fujiyoshi, Y. (1997) *Nature 389*, 206−211.

BI971701K